Aspirin-triggered resolvin D1 reduces parasitic cardiac load by decreasing inflammation through N-formyl peptide receptor 2 in a chronic murine model of Chagas disease

Short title: Aspirin-triggered resolvin D1 in Chagas disease

Ileana Carrillo[1], Rayane Rabelo[2,3], César Barbosa[2], Mariana Rates[2], Sebastián Fuentes-Retamal[1], Fabiola González-Herrera[1], Daniela Guzmán-Rivera[1,4], Helena Quintero[1], Ulrike Kemmerling[5], Christian Castillo[6], Fabiana S. Machado[2,3], Guillermo Díaz-Araya[7*], Juan D. Maya[1*]

[1]Programa de Farmacología Molecular y Clínica, ICBM, Facultad de Medicina, Universidad de Chile, Santiago, Chile

[2] Laboratório de Imunorregulação de Doenças Infecciosas, Departamento de Bioquímica e Imunologia, ICB, Universidade Federal de Minas Gerais, Belo Horizonte, Brazil

[3] Programa em Ciências da Saúde, Doenças Infecciosas e Medicina Tropical/ Laboratório Interdisciplinar de Investigação Médica, Faculdade de Medicina, Universidade Federal de Minas Gerais, Belo Horizonte, MG, Brazil

[4] Escuela de Farmacia, Facultad de Medicina, Universidad Andrés Bello, Santiago, Chile

[5]Programa de Anatomía y Biología del Desarrollo, ICBM, Facultad de Medicina, Universidad de Chile, Santiago, Chile

[6]Facultad de Medicina Veterinaria y Agronomía, Universidad de Las Américas, Santiago, Chile

[7] Departamento de Farmacología Química y Toxicología, Facultad de Ciencias Químicas y Farmacéuticas, Universidad de Chile, Santiago, Chile

*Corresponding authors

E-mail: jdmaya@uchile.cl (JDM); gadiaz@ciq.uchile.cl (GD)

ABSTRACT

Chagas disease, caused by the protozoan *Trypanosoma cruzi*, is endemic in Latin America and is widely distributed worldwide because of migration. After years of infection and in the absence of treatment, the disease progresses from an acute and asymptomatic phase to a chronic inflammatory cardiomyopathy, leading to heart failure and death. An inadequate balance in the inflammatory response is involved in the progression of chronic Chagas cardiomyopathy. Current therapeutic strategies cannot prevent or reverse the heart damage caused by the parasite. Aspirin-triggered resolvin D1 (AT-RvD1) is a pro-resolving mediator of inflammation that acts through N-formyl peptide receptor 2 (FPR2). AT-RvD1 participates in the modification of cytokine production, inhibition of leukocyte recruitment and efferocytosis, macrophage switching to a nonphlogistic phenotype, and the promotion of healing, thus restoring organ function. In the present study, AT-RvD1 is proposed as a potential therapy aid to regulate the pro-inflammatory state during the chronic phase of Chagas disease. C57BL/6 wild-type and FPR2 knock-out mice chronically infected with *T. cruzi* were treated for 20 days with 5 µg/kg/day AT-RvD1, 30 mg/kg/day benznidazole, or the combination of 5 µg/kg/day AT-RvD1 and 5 mg/kg/day benznidazole. At the end of treatment, changes in the immune response, cardiac tissue damage, and parasite load were evaluated. The administration of AT-RvD1 in the chronic phase of *T. cruzi* infection regulated the inflammatory response both at the systemic level and in the cardiac tissue, and it reduced cellular infiltrates, cardiomyocyte hypertrophy, fibrosis, and the parasite load in the heart tissue. Thus, AT-RvD1 was shown to be an attractive therapeutic due to its regulatory effect on the inflammatory response at the cardiac level and its ability to reduce the parasite load during chronic *T. cruzi* infection, thereby preventing the chronic cardiac damage induced by the parasite.

Author Summary:

Chagas disease is prevalent in Latin America and is widely distributed worldwide due to migration. If the parasite is left untreated, the disease progresses from an acute symptomless phase to chronic myocardial inflammation, which can cause heart failure and death years after infection. Imbalances in the inflammatory response are related to this progression. Current treatments cannot prevent or reverse the cardiac damage produced by the parasite. Aspirin-triggered resolvin D1, also named AT-RvD1, can modify cellular and humoral inflammatory responses leading to the resolution of inflammation, thus promoting healing and restoring organ function. In this study, AT-RvD1, in an N-formyl peptide receptor 2 (FPR2)-dependent manner, was shown to regulate local and systemic inflammation and decrease cellular infiltration in the heart tissue of mice chronically infected with the parasite and reduce cardiac hypertrophy and fibrosis. Importantly, AT-RvD1 was able to decrease parasite load in the infected hearts. Thus, this research indicates that At-RvD1 treatment is a potential therapeutic strategy that offers an improvement on current drug therapies.

Keywords: Chagas disease, cardiomyopathy, AT-RvD1, inflammation, immunomodulation, immunoregulation

Introduction

Chagas disease (CD) is caused by the protozoan *Trypanosoma cruzi*, which afflicts 7 million people in 21 endemic Latin American countries and is increasing in non-endemic countries due to migration (WHO, 2018). According to the World Health Organization [1], the most alarming statistics are that 30000 new cases, of which 8000 are newborns, are reported annually and there are more than 10000 deaths per year. Only 1% of patients receive adequate and opportune treatment. Clinically, CD initially presents an acute phase, generally asymptomatic, but in the absence of treatment a chronic phase develops. In 30% of chronic cases, patients develop cardiac or digestive complications 10-30 years after acquiring the infection [2, 3]. Chronic Chagas cardiomyopathy (CCC) is considered the most frequent and severe clinical manifestation of CD. It is characterized by focal inflammatory infiltrates, cardiac hypertrophy, and fibrosis, leading to abnormalities in the electrical conduction system and heart failure [4]. Sudden death is the leading cause of mortality in patients with CCC [5]. Chronic inflammation is considered one of the most important mechanisms involved in the pathogenesis of CD and has been proposed as a consequence of tissue damage due to the persistence of live parasites [6]. This chronic inflammation is a determining factor in the deterioration of heart architecture and loss of functionality [7]. The current treatment for CD utilizes nitroheterocyclic drugs, such as benznidazole (Bz), which are far from efficacious. For that reason, new approaches for treating this disease or improving the action of current antiparasitic drugs are needed.

Acute inflammation is a natural protective mechanism of the host in response to injury or invading pathogens. The resolution of inflammation is an active process orchestrated by molecules known as specialized pro-resolving mediators (SPM) that culminate inflammatory processes [8]. Endogenous SPMs actively participate in the dampening of host responses and the resolution of inflammation. Mainly produced by macrophages and neutrophils from distinct omega-3 polyunsaturated fatty acid pathways, the four families of SPMs, lipoxins, maresins, protectins, and resolvins, have been shown

to act as initiators of the resolution of acute inflammation; therefore, they limit polymorphonuclear neutrophil infiltration, counteract the production of cytokines and chemokines, and enhance macrophage-mediated actions [9]. Resolvin D1 (RvD1) is a novel SPM whose effects on inflammatory diseases dampen pathological inflammatory responses and restore tissue homeostasis [10]. Some drugs such as acetylsalicylic acid (ASA) modify the activity of cyclooxygenase 2 (COX-2), allowing SPM epimer generation, specifically 15-epi-LXA_4 and AT-RvD1-4 [11, 12]. These "aspirin-triggered" SPMs have the advantage of being more stable to enzymatic degradation than endogenous molecules and can serve as anti-inflammatory drugs [11, 13].

In CD, ASA has been extensively studied and beneficial effects have been reported closely related to its dose. In experimental models, a low dose of ASA (25 mg/kg) improves survival, reduces heart inflammatory infiltrates, and improves cardiac tissue architecture. These effects were associated with a significant increase in the production of 15-epi-LXA_4 [14]. Moreover, this aspirin-triggered lipoxin reduces the internalization of *T. cruzi* in macrophages [15], an effect mediated by N-formyl peptide receptor 2 (FPR2) [16, 17]. These effects have highlighted the role of FPR2 in the beneficial effects of ASA. In recent years, the effects of AT-RvD1 on CD have been reported in several publications. First, on peripheral mononuclear cells (PBMCs) from patients with stage B1 Chagas heart disease (having few cardiac abnormalities), AT-RvD1 had an immunomodulatory effect by decreasing the production of pro-inflammatory cytokines such as interferon-gamma (IFNγ) and the proliferation of PBMCs after stimulation with *T. cruzi* antigen, counteracting the inflammatory environment [18]. Second, the effect of RvD1 was recently studied in a murine model chronically infected with *T. cruzi*, where RvD1 therapy increased the survival rate and regulated the inflammatory response by reducing serum IFNγ levels and increasing serum IL-10 levels. Furthermore, RvD1 reduced inflammatory infiltrates, favoring the resolution of *T. cruzi* infection and preventing cardiac fibrosis [19].

After infection in mammals, *T. cruzi* induces robust innate and adaptive immune responses, which play a significant role during the acute and chronic phases of the disease. Nonetheless, these responses are insufficient to achieve complete clearance of the parasite, and parasite persistence promotes low and sustained inflammation over time [6]. Therefore, because of the benefits of AT-RvD1 in reducing pathological inflammatory processes and promoting restoration of tissue homeostasis, it is possible that AT-RvD1 administration in CD aids in the prevention of inflammatory damage secondary to parasite persistence and in parasite clearance. In the present study, we evaluated the effects of AT-RvD1 and whether Bz and AT-RvD1 combined therapy could improve parasite control and reduce inflammation, heart damage, and irregular cardiac electrical activity, limiting the progress of CCC in a murine model of chronic CD. Thus, we have identified AT-RvD1 as a new potential therapeutic approach to modulate the pathogenesis of CD.

Methods

Animals

Animal care and handling procedures were in accordance with the guidelines of the local animal ethics committee. Eight to ten-week-old C57BL/6 wild-type (WT) mice were obtained from the Animal Care Facilities of Universidade Federal de Minas Gerais (UFMG, Brazil). The FPR2 knockout mice were bred on a C57BL/6 genetic background under pathogen-free conditions at the Instituto de Ciências Biológicas – UFMG. The animals were randomly distributed and were housed at 2 to 3 animals per box in a controlled environment at constant temperature, under a 12-h day/night cycle, and with food and water available *ad libitum*. This research study was carried out in strict accordance with the Brazilian Guidelines on animal work and the Guide for the Care and Use of Laboratory Animals of the National Institutes of Health (NIH). The Institutional Bioethics Committee of the Faculty of Medicine, University of Chile, approved the supervising protocols (Protocol CBA# 1078 FMUCH, associated with FONDECYT-Chile grant number 1170126).

Parasites and infection protocols

Dm28c trypomastigotes from Vero cell cultures (1×10^5) were used to intraperitoneally inoculate the C57Bl/6 mice. At the peak of parasitemia, blood was collected and pooled from various donors, and the parasites were counted by direct visualization of a drop of blood under a light microscope. Finally, the trypomastigotes were suspended in sterile saline, and 1×10^3 trypomastigotes in 100 µL were injected into each experimental animal. After randomization, the animals were divided into five groups (healthy groups) or eight groups (infections and different treatments). *T. cruzi* infection was confirmed from the third day after infection by direct microscopic visualization of circulating trypomastigotes in peripheral blood samples obtained from the tail tip. Subsequently, the parasitemia was monitored every two days via peripheral blood samples until undetectable [14].

Treatment protocols

Infected C57BL/6 WT and FPR2$^{-/-}$ mice were treated with 5 µg/kg/day aspirin-triggered Resolvin D1 (AT-RvD1) (Cayman Chemicals®, Ann Harbor, MI, USA), 30 mg/kg/day Bz (Abarax - Elea Laboratory, Buenos Aires, Argentina), or a combination of 5 µg/kg/day AT-RvD1 + 5 mg/kg/day Bz. The Bz was suspended in 0.5% carboxymethylcellulose and administered orally once a day. AT-Rv1 was dissolved in 0.01% ethanol and administered intraperitoneally once a day. The treatments were administered from day 40 to 60 post-infection (p.i.). On day 60 p.i., the animals were anesthetized with 100 mg/kg ketamine and 10 mg/kg xylazine, and their blood and hearts removed. The hearts were halved, with one half fixed in 4% formaldehyde in 0.1 M phosphate-buffered saline (PBS; pH 7.3) for histological analysis and the other half extracted in TRIzol™ (Invitrogen, Waltham, MA, USA) for mRNA expression analysis by RT-qPCR.

Enzyme-linked immunosorbent assay (ELISA)

Peripheral blood was collected from the submandibular vein of the C57BL/6 mice on days 20 and 40 p.i. On day 60, whole blood was collected after euthanasia. The blood was centrifuged, and the resulting serum was stored at -80 °C. Cytokine quantification was performed on the serum samples by ELISA using specific mouse monoclonal antibodies from the ELISA Max Deluxe Set for mouse tumor necrosis factor alpha (TNFα), IFNγ, interleukin (IL)-1β, and IL-10 (BioLegend, San Diego, CA, USA), following the manufacturer's instructions. The absorbance of the ELISA plate wells was read at 450 nm in a microplate reader Biotek® (Winooski, VT, USA). All samples were analyzed in duplicate.

Quantitative reverse transcription PCR (RT-qPCR) assay

For measurements of cytokine gene expression in cardiac tissue, total RNA was isolated using TRIzol™ reagent, followed by DNAse treatment and purification using the PureLink RNA Mini Kit (Thermo Fisher Waltham, MA, USA) according to the manufacturer's instructions. cDNA was synthesized from 600 ng of total RNA by reverse transcription using M-MLV reverse transcriptase

and random primers (Invitrogen). For the qPCR analyses, each reaction mix contained 150 nM of each primer (forward and reverse), 1 ng of sample cDNA, 7 µL of SensiMix™ SYBR® Green Master Mix (Bioline®, Memphis, TE, USA), and H_20 in a total volume of 15 µL. The primers used for the analysis of cytokines and hypertrophy markers were the following: TNFα, Fw: 5′-TAGCCCACGTCGTAGCAAAC-3′ and Rv: 5′-ACAAGGTACAACCCATCGGC-3′; IFNγ, Fw: 5′-AACTGGCAAAAGGATGGTGAC-3′ and Rv: 5′-TTGCTGATGGCCTGATTGTC-3′; IL-1β, Fw: 5′-TGCCACCTTTTGACAGTGATG-3′ and Rv: 5′-GTGCTGCTGCGAGATTTGAA-3′; IL-10, Fw: 5′-ACCTGGTAGAAGTGATGCCC-3′ and Rv: 5′-ACAGGGGAGAAATCGATGACAG-3′; atrial natriuretic peptide (ANP), Fw: 5′-GGGCTTCTTCCTCGTCTTGG-3′ and Rv: 5′-GTGGTCTAGCAGGTTCTTGAAAT-3′; brain natriuretic peptide (BNP), Fw: 5′-CAGAGCAATTCAAGATGCAGAAGC-3′ and Rv: 5′-CTGCCTTGAGACCGAAGGAC-3′. The amplification was performed in an ABI Prism 7300 sequence detector (Applied Biosystems®, Waltham, MA, USA). The cycling program was as follows: a denaturation step at 95 °C for 3 min and 40 amplification cycles of 95 °C (15 s), 60 °C (15 s), and 72 °C (30 s). The final step was a dissociation stage that ramped from 60 to 95 °C over 100 s. For relative quantification, the results were expressed as RQ values determined using the comparative control (delta-delta-Ct (DDCt)) method [20].

The presence of viable parasites in cardiac tissue was evaluated by amplification of 18S *T. cruzi* ribosomal RNA (rRNA). For this purpose, total RNA was isolated using TRIzol™ and purified using the PureLink RNA Mini Kit; cDNA was synthesized as detailed above. RT-qPCR was performed as described above with the following primers: 18S, Fw: 5′-TGGAGATTATGGGGCAGT-3′ and Rv: 5′-GTTCGTCTTGGTGCGGTCTA-3′. The parasitic load of *T. cruzi* in the cardiac tissues was calculated from a standard curve constructed using 1×10^8 trypomastigotes of *T. cruzi*, serially diluted to provide a log curve in the range of 1 to 10^8 equivalent parasites/10 ng of tissue RNA.

224 Histology

225 The hearts from the euthanized mice were fixed in 4% formaldehyde (pH 7.3). Then, the fixed heart
226 tissues were dehydrated with 50 to 100% ethanol, clarified with xylol, embedded in paraffin, and
227 sectioned in 5 μm slices. The sections were stained with hematoxylin and eosin to observe cellular
228 infiltration and cardiomyocyte cross-sectional area or with picrosirius red to observe collagen
229 organization. Images were obtained using a spinning-disk microscope (Olympus BX42). Five fields
230 per heart (40X) were analyzed using Image J software.

231 For the analysis of cellular infiltrates, the nuclei present in five fields of each heart were quantified.
232 The number of nuclei per tissue area was counted in order to eliminate empty tissue areas. In the
233 analysis of cardiomyocyte cross-sectional area, only muscle fibers with well-defined borders and a
234 nucleus inside were included. For the analysis of fibrosis in the picrosirius red-stained slides, the
235 red-colored pixels in the cardiac tissue were quantified in five fields per animal.

236 Electrocardiogram (ECG) recording and analysis

237 ECG recording was performed using a six-channel non-invasive electrocardiograph (ECG-PC
238 version 2.07, Electronic Technology of Brazil (TEB), Belo Horizonte/MG, Brazil). The mice were
239 anesthetized initially with 2.5% isoflurane and then maintained with 1.5% isoflurane (VetCase-
240 Incotec, Serra/ES, Brazil). The mice were placed in a dorsal recumbent position on a wooden table
241 covered with plastic material; electrocardiographic gel was applied, and four alligator clip
242 electrodes were attached to the skin of the forelimbs and hindlimbs. All procedures were performed
243 in a quiet room to minimize stress.

244 All ECGs were performed and analyzed by the same technician according to standard methods for
245 ECG trace analysis. The tracings were recorded from six leads of the frontal plane at a velocity of
246 50 mm/s. In each tracing, three segments containing five beats (lead II) were selected for quality
247 (clean baseline with no artifacts), and the mean values for heart rate (HR) and duration of the

intervals and waves were determined. The parameters evaluated were heart rate, P wave, QRS complex, PR interval, and QT interval. QT-corrected values were obtained from Bazett's formula.

Statistical analysis

For all experiments, statistical significance was established at p values of 0.05. The data represent the means ± standard deviations (SD) from at least three independent observations or experiments. All statistical analyses were performed using GraphPad Prism 8.0 software. One-way and two-way analyses of variance (ANOVAs) (with Tukey's post-hoc tests) were performed as appropriate. A log-rank test was performed for survival analysis.

Results

Effect of the absence of FPR2 on *T. cruzi* parasitemia

The progression of parasitemia and mortality in C57BL/6 WT and FPR2$^{-/-}$ mice infected with *T. cruzi* strain Dm28c were determined to evaluate the establishment of a murine model for chronic CD (Fig 1). As expected, in the WT mice, detectable parasitemia persisted for approximately 40 days, with the peak of infection occurring at 27 days p.i. (Fig 1A). In the FPR2$^{-/-}$ mice, the parasitemia level was significantly lower in the second peak of infection, but the overall kinetics during the acute phase was similar to that of the WT mice.

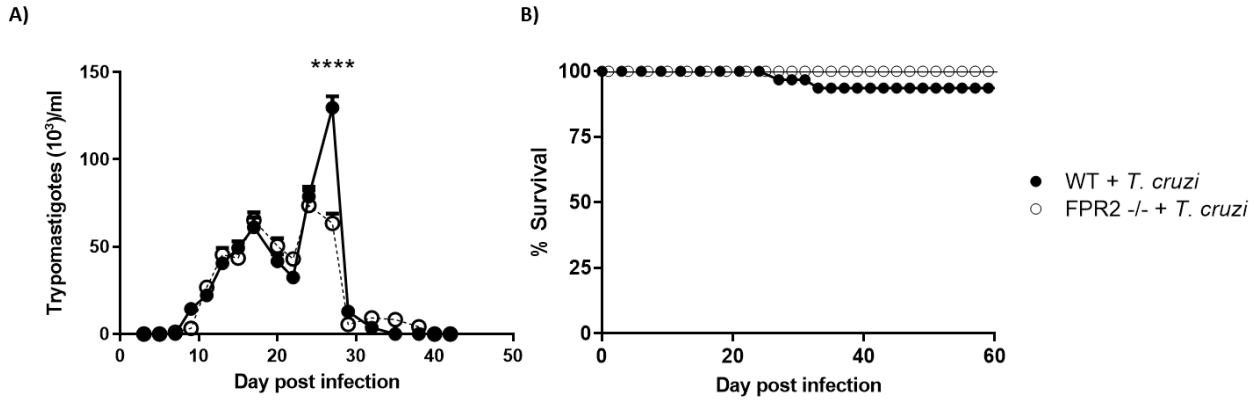

Fig 1. Parasitemia and survival in C57BL/6 wild-type (WT) or FPR2 knock-out (FPR2 -/-) mice infected with *Trypanosoma cruzi* (Dm28c). A) Blood parasite levels, B) Kaplan-Meier survival curves. Data are expressed as the mean ± SD (n = 8). Two-way ANOVA was performed to identify significant differences, ****$p \leq 0.0001$.

Furthermore, survival rates were high for all mice until the end of the experiment, regardless of their genetic background, confirming that the mortality of this murine model of *T. cruzi* chronic infection was low.

Regarding inflammatory responses, changes in serum levels of pro-inflammatory (TNFα, IFNγ, IL-1β) and anti-inflammatory cytokines (IL-10) were determined at days 20, 40, and 60 p.i. in WT and FPR2$^{-/-}$ mice infected with *T. cruzi* (S1 A, C, E, and G Fig). Both the healthy WT and FRP2$^{-/-}$ mice showed differences in serum cytokine levels at baseline and after *T. cruzi* infection. The healthy FPR2$^{-/-}$ mice had elevated levels of TNFα and IL-10 compared to those of the healthy WTs (S1 A and G Fig). In addition, the magnitude of the inflammatory response was higher in the WT mice than in the FPR2$^{-/-}$ mice (S1B, D, and H Fig). At day 40 p.i., the infected WT mice still maintained slightly increased TNFα, IFNγ, and IL-10 levels compared to their healthy controls, while the FPR2$^{-/-}$ mice only had slightly increased IFNγ levels. These findings indicate that the FPR2$^{-/-}$ mice developed a different immune response against *T. cruzi* infection than the WT mice (S1 Fig).

285 Effect of AT-RvD1 treatment on the inflammatory state in CD

286 The effect of AT-RvD1 treatment on inflammation in chronic CD was evaluated by measuring
287 serum cytokine levels at the end of treatment (60 dpi). Consistent with a chronic inflammatory state,
288 the serum levels of pro-inflammatory cytokines such as TNFα (Fig 2A), IFNγ (Fig 2B), and IL-1β
289 (Fig 2C) increased as a result of the infection in the WT and FPR2$^{-/-}$ mice, although the IL-1β
290 increase in the FPR2$^{-/-}$ mice was not significant. Unexpectedly, AT-RvD1 did not reduce serum
291 TNFα levels in the WT mice (Fig 2A); however, AT-RvD1 treatment significantly reduced the
292 serum levels of IFNγ (Fig 2B) and IL-1β (Fig 2C), reaching healthy control levels. This effect was
293 mediated by FPR2 because in the FPR2$^{-/-}$ mice, AT-RvD1 treatment did not alter IFNγ levels. In
294 contrast, Bz, alone or combined with AT-RvD1, did not affect the increased serum levels of pro-
295 inflammatory cytokines, except for IL-1β in the WT mice (Fig 2C). Either treatment produced
296 negligible effects on Il-10 (Fig 2D).

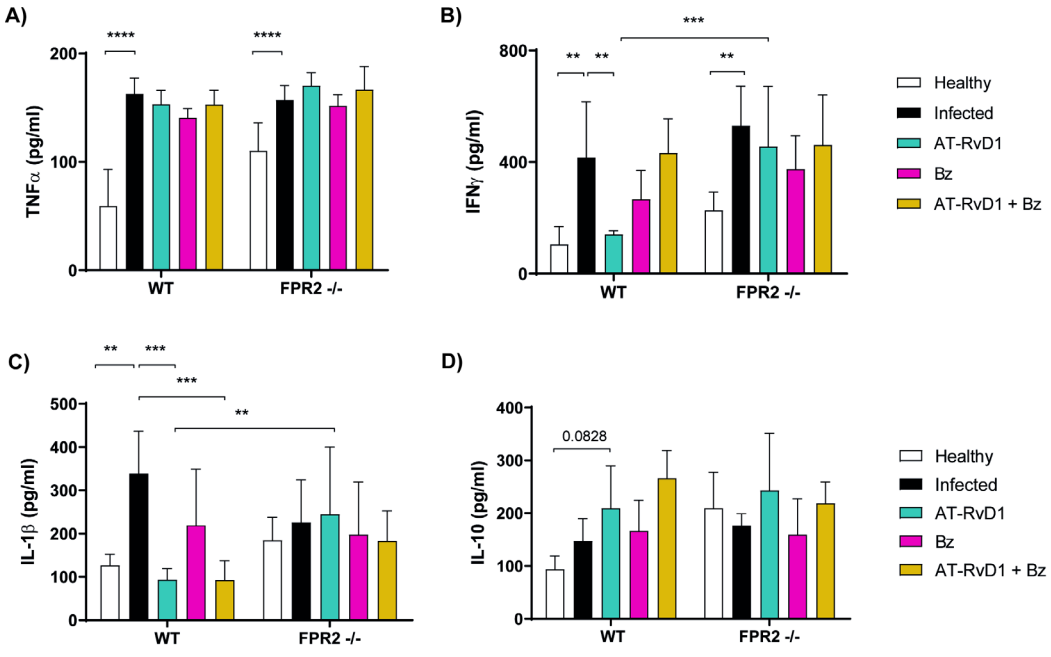

297

298 **Fig 2. Serum cytokine levels in mice infected with *Trypanosoma cruzi* and treated with AT-**
299 **RvD1 and/or Bz at 60 days post-infection.** The concentrations of TNFα (A), IFNγ (B), IL-1β (C),

and IL-10 (D) in serum were quantified by ELISA. Data are expressed as the mean ± SD (n = 5). Two-way ANOVAs and Tukey's post-hoc tests were performed to identify significant differences. **p ≤ 0.01, ***p ≤ 0.001, ****p ≤ 0.0001. Bz, benznidazole; AT-RvD1, aspirin-triggered resolvin D1.

Because serum cytokine levels reflect systemic inflammatory states, it was also necessary to measure them in the heart to determine local inflammatory states. Thus, the effect on the immune response in cardiac tissue was determined by measuring relative cytokine mRNA levels after 20 days of treatment with AT-RvD1 (60 dpi). In this case, mRNA levels of the pro-inflammatory TNFα (Fig 3A), IFNγ and IL-1β (Fig 3C) cytokines were increased in both the WT and FPR2$^{-/-}$ infected mice. Although the mRNA levels of IFNγ were exceedingly increased with the infection, it was not modified by At-RvD1 or Bz in WT and FPR2$^{-/-}$ mice (Fig 3B). Interestingly, in the WT and FPR2$^{-/-}$ mice, AT-RvD1 treatment significantly increased IL-10 expression levels (Fig 3D). AT-RvD1 prevented the increase in TNFα caused by infection. Neither Bz nor combinatorial therapy modified the mRNA levels of the measured cytokines.

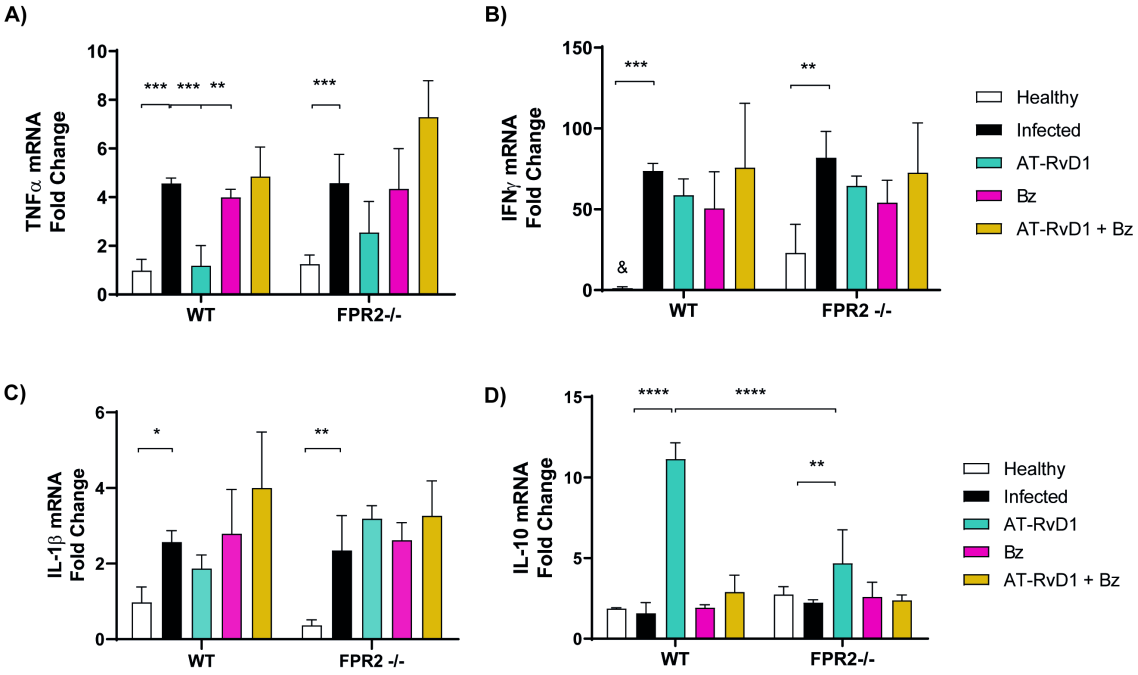

Fig 3. Cytokine mRNA levels in cardiac tissue of mice infected with *Trypanosoma cruzi* and treated with AT-RvD1 or Bz at 60 days post-infection. The cardiac mRNA levels of TNFα (A), IFNγ (B), IL-1β (C), and IL-10 (D) are shown from uninfected C57BL/6 mice infected with *T. cruzi* and treated with AT-RvD1 and Bz, as assessed by RT-qPCR. Data are expressed as the mean ± SD (n = 5). Two-way ANOVAs and Tukey's post-hoc tests were performed to identify significant differences. *p ≤ 0.05, **p ≤ 0.01, ***p ≤ 0.001, ****p ≤ 0.0001. & indicates indeterminate values. Bz, benznidazole; AT-RvD1, aspirin-triggered resolvin D1.

In CCC, chronic inflammation is a determining factor in the deterioration of heart architecture. The cellular infiltrates in heart tissue sections were measured to evaluate the effect of AT-RvD1 treatment on cardiac inflammation. Histological analysis of cardiac tissue stained with hematoxylin-eosin was performed, and cellularity was quantified (Fig 4A). WT and FPR2$^{-/-}$ mice infected with *T. cruzi* (60 dpi) showed focal inflammatory infiltrates and increased cellularity in cardiac tissue. AT-RvD1 significantly reduced focal inflammatory infiltrates in the cardiac tissue (Fig 4B); the absence of FPR2 impaired the reduction in cellular infiltrates, suggesting that this receptor mediates the AT-

RvD1 effect. Moreover, the effect of AT-RvD1 in reducing the inflammatory infiltrates had a higher significance level than that obtained with Bz alone. Consistently, the combination of AT-Rv1 with Bz significantly reduced the inflammatory infiltrates in the WT mice, whereas, in the absence of FPR2, the reduction in inflammatory infiltrates achieved by combinatorial therapy was probably dependent on the effect of Bz.

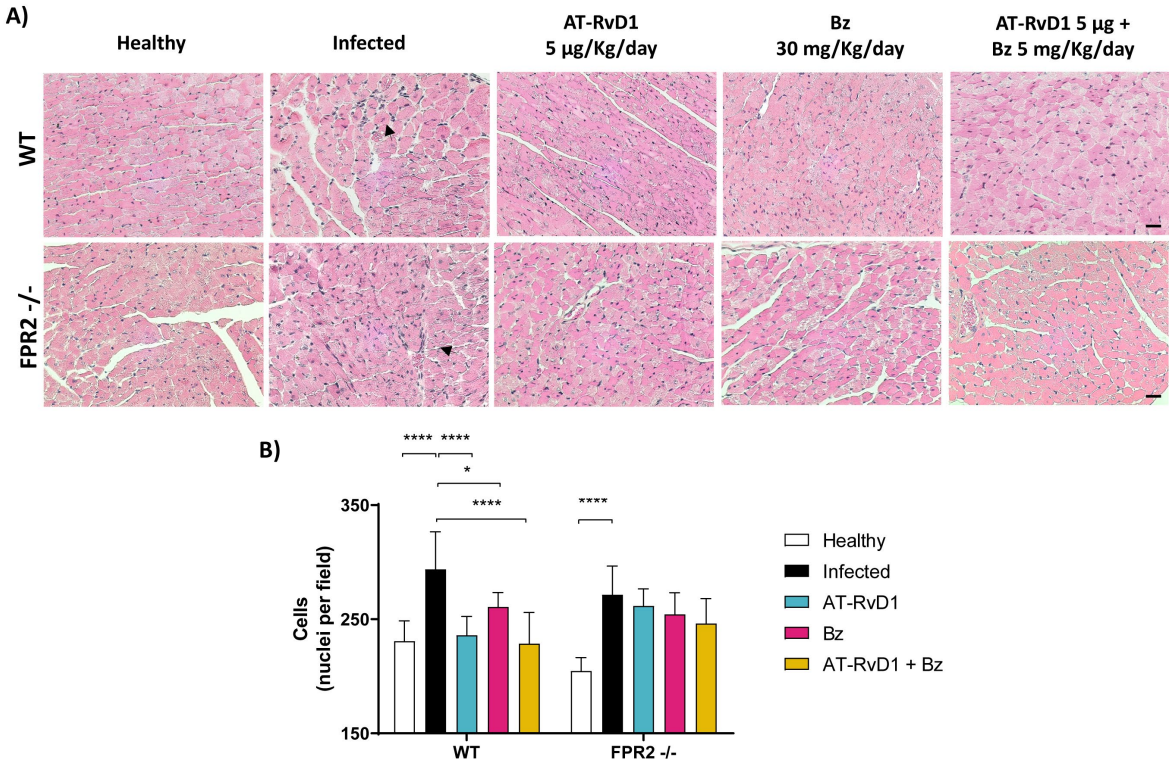

Fig 4. AT-RvD1 reduces cellular infiltrates in the heart tissue of C57BL/6 mice chronically infected with *Trypanosoma cruzi*. A) Representative images of heart tissue stained with hematoxylin and eosin from C57BL/6 mice infected with *T. cruzi* and treated with AT-RvD1 or benznidazole (Bz) at the indicated doses. Black arrows show infiltrated cells. Scale bar = 20 µm. B) Quantitative analysis of cellularity in cardiac tissues from five fields per animal. Data are expressed as the mean ± SD (n = 8). A two-way ANOVA and Tukey's post-hoc tests were performed to

identify significant differences. *p ≤ 0.05, ****p ≤ 0.0001. AT-RvD1, aspirin-triggered resolvin D1.

Through FPR2, AT-RvD1 prevents cardiac remodeling in chronic CD

Because cardiac hypertrophy and dysfunction are significant complications of CCC, the effect of AT-RvD1 on cardiac hypertrophy was assessed by measuring the cross-sectional area of cardiomyocytes from heart tissue sections stained with hematoxylin-eosin (Fig 5A). *T. cruzi* infection increased the cross-sectional area of cardiomyocytes in the WT and FPR2$^{-/-}$ mice after 60 dpi, demonstrating structural changes in the earliest phases of chronic disease. It is striking that in healthy FPR2$^{-/-}$ mice, the cross-sectional areas were also increased compared with those in the WT mice, which was consistent with the overall increase in circulating cytokine levels (Fig 2). Although AT-RvD1 significantly reduced cardiomyocyte cross-sectional area, the effect was blunted by the absence of FPR2 because in the FPR2$^{-/-}$ mice, there was no reduction in cardiac hypertrophy (Fig 5B). It is important to note that Bz alone did not affect cardiac hypertrophy; however, when combined with AT-RvD1, it significantly reduced the cross-sectional area of cardiomyocytes in the WT mice, but not in the absence of FPR2. These results suggest that AT-RvD1 therapy can reduce cardiac hypertrophy. These observations were supported by measuring the mRNA levels of ANP and BNP, molecular markers of cardiac hypertrophy (Fig 5C and D, respectively). Both ANP and BNP were significantly increased in the infected WT and FPR2$^{-/-}$ mice (60 dpi), although the changes in the FPR2$^{-/-}$ mice were negligible. Consistent with the histological analyses, treatment with AT-RvD1 significantly reduced both molecular markers of cardiac hypertrophy. However, the absence of FPR2 did not change the effect of AT-RvD1, suggesting that an alternative way mediated this effect. Bz alone or combined with AT-RvD1 did not modify these molecular markers of hypertrophy.

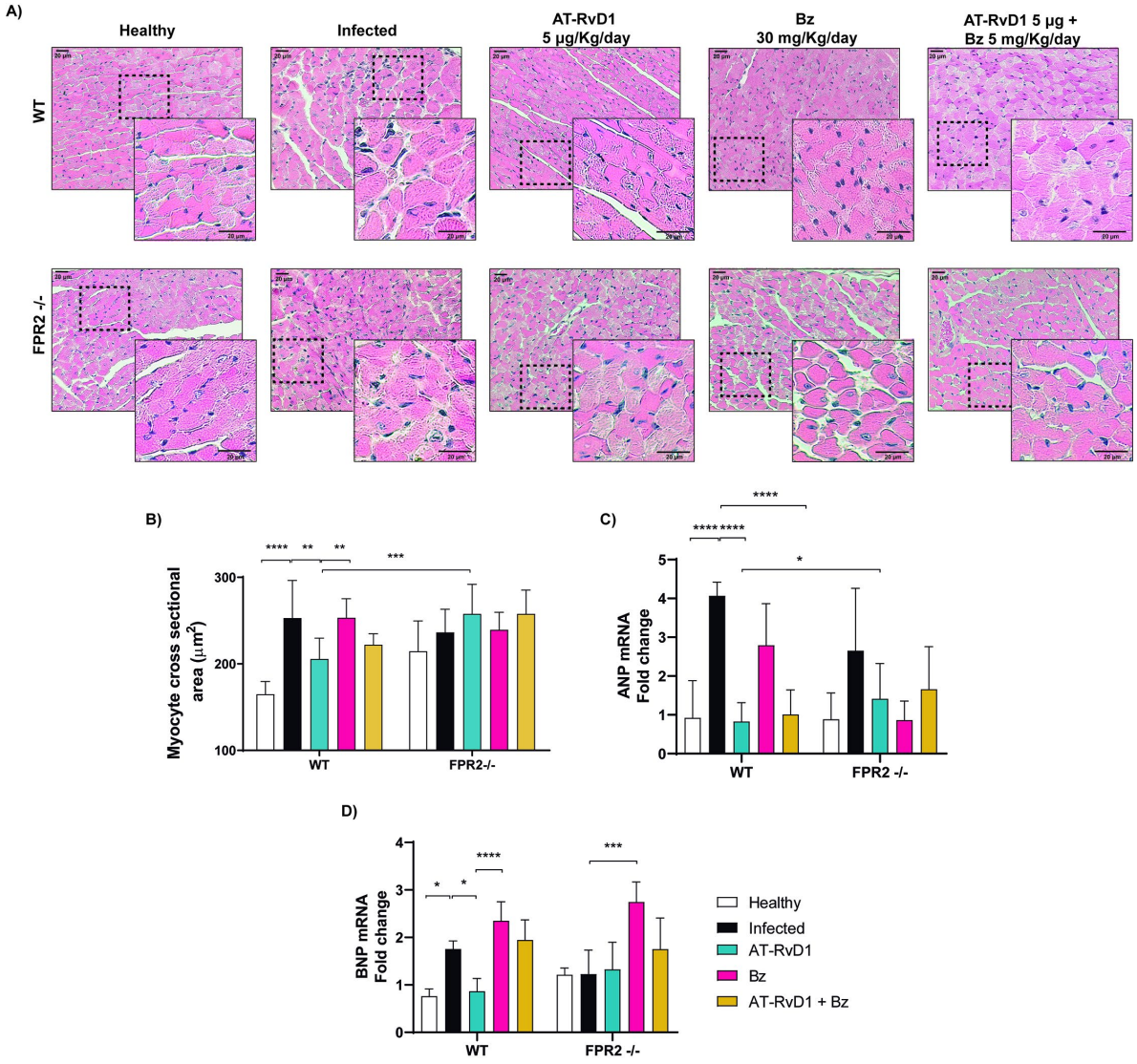

Fig 5. AT-RvD1 reduces cardiac hypertrophy in C57BL/6 chronically infected with *Trypanosoma cruzi*. A) Images are enlargements of the representative images shown in Fig 4. B) Analysis of the cross-sectional area of cardiomyocytes; 200 cardiomyocytes were randomly chosen per animal. Scale bar = 20 µm. C, D) mRNA levels of atrial natriuretic peptide (ANP) and brain natriuretic peptide (BNP), as markers of hypertrophy, are shown from cardiac tissue of C57BL/6 mice infected with *T. cruzi* and treated with AT-RvD1 and/or Bz, as measured by RT-qPCR. Data are expressed as the mean ± SD (n = 5). Two-way ANOVAs and Tukey's post-hos tests were

376 performed to identify significant differences. *p ≤ 0.05, **p ≤ 0.01, ***p ≤ 0.001, ****p ≤ 0.0001.
377 Bz, benznidazole; AT-RvD1, aspirin-triggered resolvin D1.

378

379 Although cardiac hypertrophy in chronic CD is a hallmark of cardiac remodeling, cardiac fibrosis
380 reflects more profound structural damage. Thus, the effect of AT-RvD1 on cardiac fibrosis in CCC
381 was analyzed in cardiac tissue stained with picrosirius red to visualize collagen fibers (Fig 6A).
382 Consequently, cardiac fibrosis was increased with CD progression in both WT and FPR2$^{-/-}$ infected
383 mice (60 dpi), and AT-RvD1 significantly reduced this cardiac fibrosis more efficiently than Bz in
384 both genotypes.

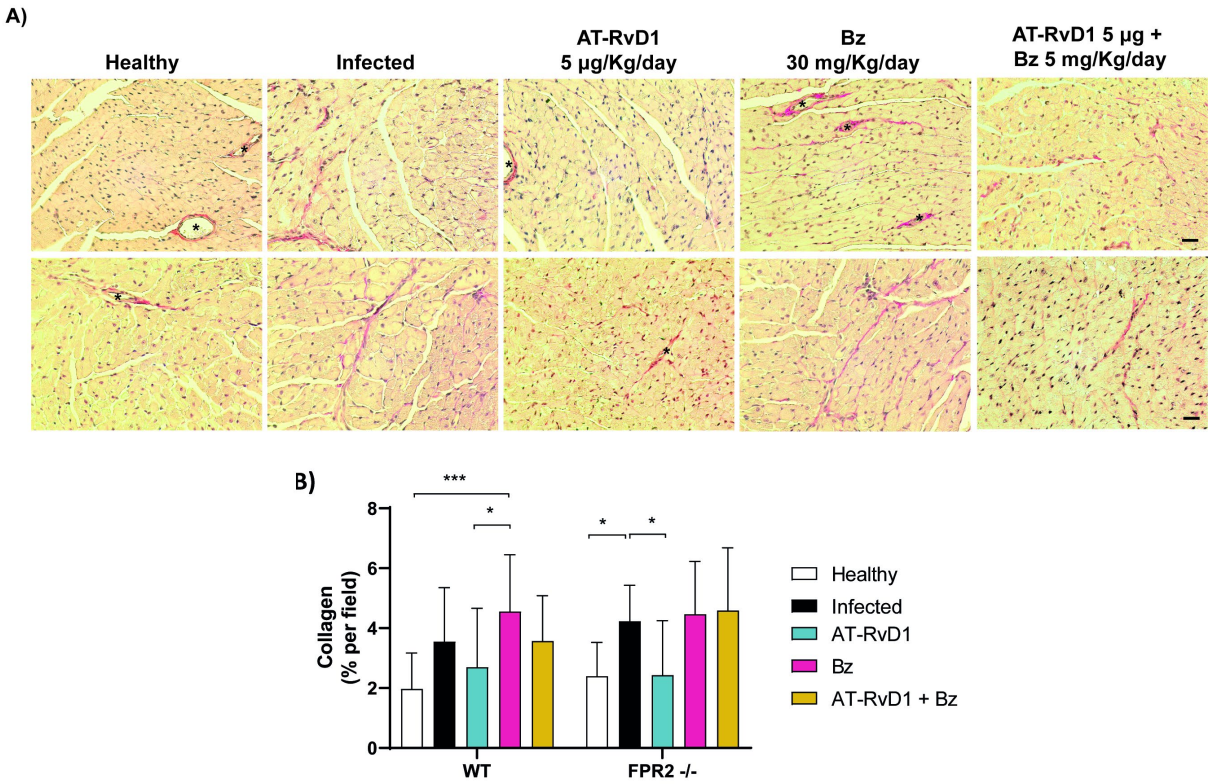

385

386 **Fig 6. AT-RvD1 reduces cardiac fibrosis in C57BL/6 mice chronically infected with**
387 ***Trypanosoma cruzi*.** A) Representative images of picrosirius red-stained heart tissue from C57BL/6
388 mice infected with *T. cruzi* (Dm28c) and treated with AT-RvD1 or benznidazole (Bz) at the

indicated doses. Asterisks show blood vessels. Scale bar = 20 μm. B) Quantitative analysis of red pixels in the stained cardiac tissue, corresponding to regions of fibrosis, from five fields per animal. Data are expressed as the mean ± SD (n = 8). A two-way ANOVA and Tukey's post-hoc tests were performed to identify significant differences. *$p \leq 0.05$, ***$p \leq 0.001$. AT-RvD1, aspirin-triggered resolvin D1.

Signs of cardiac remodeling include atrioventricular and intraventricular conduction disorders such as right bundle branch block, sinus bradycardia, and QT interval changes, alterations that may occur early p.i. [21, 22]. Thus, the electrocardiographic activities of the C57BL/6 WT and FPR2$^{-/-}$ mice were evaluated at the end of the treatments. However, at 60 dpi, no significant changes were found in the ECG parameters of the mice (S2 Fig).

AT-RvD1 reduces parasite load in chronic CD

Cardiac parasite load was determined to verify establishment of the chronic phase and impact of the treatments on parasite clearance. For this determination, RT-qPCR of *T. cruzi* 18S rRNA was performed to determine parasite numbers in the cardiac tissue at the end of the treatments. As expected, Bz reduced cardiac *T. cruzi* load to undetectable levels in both the WT and FPR2$^{-/-}$ mice (Fig 7). However, a surprising finding was that AT-RvD1 decreased the cardiac *T. cruzi* load in the WT and FPR2$^{-/-}$ mice, although the decrease in parasitic load was less marked in the null mice. This finding was unexpected because AT-RvD1 does not have trypanocidal properties.

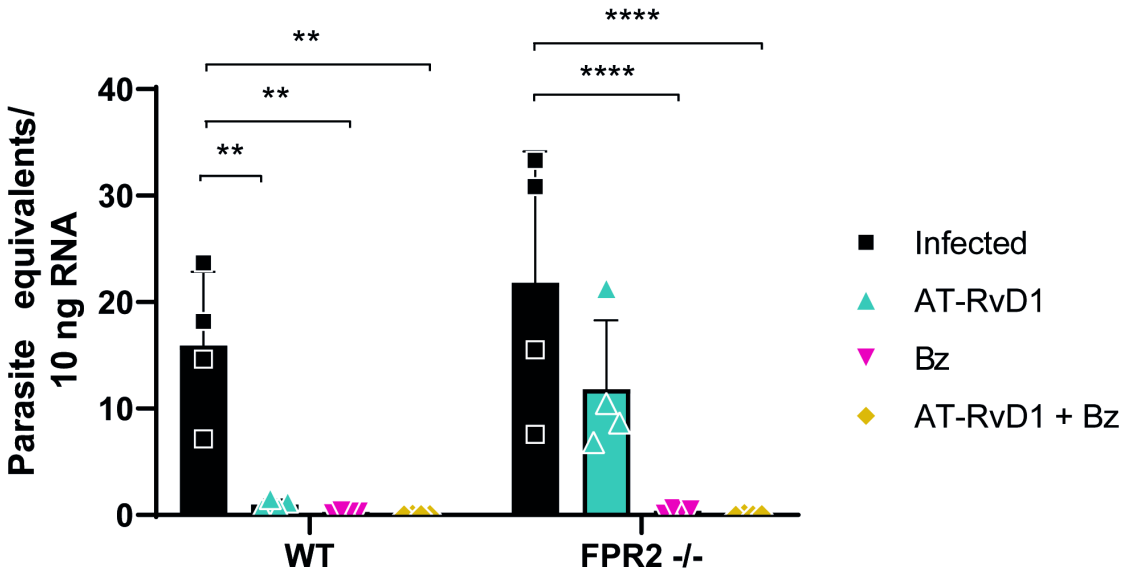

Fig 7. Parasite load in cardiac tissue of mice chronically infected with *Trypanosoma cruzi* and treated with AT-RvD1 and/or Bz at 60 dpi. 18S rRNA from *T. cruzi* was detected by RT-qPCR. Data are expressed as the mean ± SD (n = 4). Two-way ANOVA and Tukey's post-hoc tests were performed to identify significant differences. **p ≤ 0.01, ****p ≤ 0.0001. Bz, benznidazole; AT-RvD1, aspirin-triggered resolvin D1.

Discussion

Involvement of inflammation resolution in parasitemia control

In the experimental model used, the course of parasitemia in the WT mice was representative of the behavior expected by the Dm28c strain of *T. cruzi* [14, 23]. In contrast, the FPR2$^{-/-}$ mice showed a decrease in parasitemia. The latter results are consistent with other experimental models where the deletion of 5-lipoxygenase (5-LO), which participates in the biosynthesis of lipoxins, also developed reduced parasitemia [24, 25]. However, in other studies, 5-LO deficiency led to increased parasitemia without affecting survival or infection control [26, 27]. These results suggest

that the breakdown of one or more pro-resolving elements of inflammation allows better control of the parasite during the acute phase of the disease. This is probably caused by less containment of the inflammatory response and an increased macrophage capability to eliminate parasites. Specifically, parasitemia in the FPR2$^{-/-}$ mice was reduced after three weeks p.i., the time when an adaptive antigen-specific response is established and cytotoxic and helper T lymphocytes and B cells participate [28]. These responses could be more efficient in the FPR2$^{-/-}$ mice.

The WT and FPR2$^{-/-}$ mouse survival was similar and elevated throughout the experimental timeline, probably because the C57BL/6 mouse lineage is resistant to infection with *T. cruzi* [29]. Interestingly, healthy FPR2$^{-/-}$ mice had elevated basal levels of IL-10 (S1 Fig), which could be related to a lower risk of mortality during the acute phase of infection. In contrast, infected IL-10 knockout mice have a poor survival rate [30]. Thus, the anti-inflammatory balance mediated by IL-10 likely plays a fundamental role in the survival and control of deleterious inflammatory responses, probably mediated by Treg cell functions [25, 31].

The transition from acute to chronic phase is accompanied by decreased tissue parasitism and blood parasitemia and control of the inflammatory response [32], which was observed in our experimental model at 40 p.i.

AT-RvD1 decreases the inflammatory process in chronic CD

Our results showed that infection with *T. cruzi* triggers a robust inflammatory response in the acute phase, with the production of inflammatory cytokines, such as IFNγ and TNFα, which have been shown to activate macrophages to eliminate the parasite [32]. At day 60 p.i., the WT mice showed slightly increased but sustained levels of the pro-inflammatory cytokines TNFα, IFNγ, and IL-1β, reflecting an inflammatory state in the early stages of chronicity. Treatment with AT-RvD1 during the early chronic phase significantly reduced the serum levels of IFNγ and IL-1β, producing an immunoregulatory effect of the inflammatory state at the systemic level. These results are consistent

with previous studies, which have shown that PBMCs obtained from chagasic patients in stage B1 (the initial stage of CCC) treated with AT-RvD1 had lower IFNγ production than after antigenic re-exposure to *T. cruzi*, and their cell proliferation was reduced, highlighting the immunomodulatory effect of AT-RvD1 [18].

At the cardiac level, the scenario against *T. cruzi* is not very different. An imbalance is found, with high levels of pro-inflammatory cytokines (TNFα, IFNγ, and IL-1β) and practically unchanged levels of anti-inflammatory cytokines (IL-10). This could reflect the cell populations (including macrophages, cytotoxic T lymphocytes, and helper T lymphocytes) infiltrating the cardiac tissue to coordinate parasite control and represents an exacerbated production of cytokines related to tissue destruction [6]. However, the participation of other cardiac cells such as fibroblasts, endothelial cells, and cardiomyocytes has not been excluded [33]. Moreover, treatment with AT-RvD1 generates an immunomodulatory effect by drastically reducing the production of TNFα at the cardiac level and suddenly increasing the production of IL-10. This suggests that AT-RvD1 increases the proportion of IL-10-producing cells (macrophage subpopulations, Treg and Breg cells) in cardiac tissue to regulate the inflammatory environment.

Furthermore, the decrease in TNFα production may be secondary to the increase in IL-10 because the latter is a potent inhibitor of TNFα mRNA expression through activation of the STAT3 transcription factor pathway in human monocytes and macrophages [34]. That would also explain why, at the systemic level, we did not observe a reducing effect of TNFα. High levels of IL-10 have been associated with evasion of the immune response by different pathogens, including *T. cruzi* [35], contributing to increased mortality or persistence of damage [36]. However, high IL-10 levels can also decrease inflammation and pathology; consequently, a pro/anti-inflammatory balance is necessary for the natural evolution of the disease [37]. Nevertheless, elevated levels of IL-10 seem to be related to maintaining adequate cardiac function in indeterminate patients with CD [38-40]. Therefore, the AT-RvD1 effect on IL-10 production in the heart appears to be beneficial for

preventing CCC progression since changes in IL-10 levels have been associated with losing the ability to control the inflammatory immune response.

Although IFNγ is produced in the heart tissue by Th1 cell infiltrates in CCC, there was no change in the mRNA of this cytokine after AT-RvD1 treatment. This finding does not correlate with the corresponding IFNγ serum levels. However, AT-RvD1 reduced the inflammatory infiltrate in cardiac tissue and was more efficient than Bz alone, probably mediated by reduced cellular and vascular adhesion molecules (VCAM, ICAM) [41-43] in conjunction with modulation of the inflammatory environment, as discussed above.

Previous studies have shown that the anti-inflammatory and pro-resolving properties of AT-RvD1 are primarily mediated by FPR2 [43]. In our model, FPR2 plays a fundamental role in regulating pro-inflammatory and anti-inflammatory cytokines (IFNγ and IL-1B) and reducing cellular infiltrates because its absence weakens the effect produced by AT-RvD1. Although the mechanism of action of RvD1 is not fully understood, it has been shown to exert its anti-inflammatory effects by inhibiting the NF-κB pathway [44, 45], suppressing cytosolic calcium, and decreasing activation of the calcium-sensitive kinase calcium-calmodulin-dependent protein kinase II (CaMKII) [46].

Previous studies have shown that Bz, in addition to its trypanocidal properties, reduces cardiac cell infiltrates and the production of inflammatory mediators via inhibition of the NF-κB pathway [5, 47-49], apparently, an effect dependent on IL-10 [50]. However, in the chronic CD model presented herein, Bz did not regulate production of the pro-inflammatory (TNFα, IFNγ, and IL-1β) and anti-inflammatory (IL-10) cytokines studied. Thus, there was only a slight reduction in the inflammatory infiltrates with Bz treatment. Moreover, the combination of 5 mg/kg Bz and 5 μg/kg AT-RvD1 reduced cardiac inflammatory infiltrates but did not modulate the pro- and anti-inflammatory cytokines studied. Unfortunately, no synergistic or additive effect could be observed between the two drugs. Although both drugs act by inhibiting the NF-κB pathway, Bz could also increase

reactive oxygen species production at the tissue level [51, 52], contributing to the production and establishment of a pro-inflammatory environment. This possibly explains why, although Bz is effective as a trypanocidal therapy, it does not reduce the cardiovascular events observed in patients with CCC [53].

The most recurrent lesion in advanced CCC is fibrosis and wall thinning, consistent with dilated cardiomyopathy. Cardiomyocyte loss, due to parasite persistence and the consequent inflammatory process, is characteristic of myocarditis, which is much less intense in indeterminate patients. Here, cardiomyocyte hypertrophy was observed, evidenced by an increase in cell cross-sectional area and correlated with elevated levels of natriuretic peptides, indicating hemodynamic overload. Together with the interstitial fibrosis observed, these findings point to the presence of myocarditis characteristic of CCC [7].

To the best of our knowledge, until now, the effect of AT-RvD1 on hypertrophy produced by infection with *T. cruzi* had not been studied. Herein, AT-RvD1 was shown to reduce both the cross-sectional area of cardiomyocytes and the transcription of hypertrophy markers such as ANP and BNP, which have been associated with different stages and severity of CCC [54, 55]. Furthermore, during *T. cruzi* infection, the participation of endothelin-1, cardiotrophin-1, and cytokines such as TNFα and IL-1β has been previously highlighted as pro-hypertrophic [56]. Therefore, the effect of AT-RvD1 on hypertrophy could also be a consequence of its immunoregulatory effect [57]. Although FPR2 mediates the anti-hypertrophic effect of AT-RvD1, it also activates G protein-coupled receptor 23 (GPR23) [58]. Thus, GPR32 participation may be an alternative pathway for the action of AT-RvD1, explaining the changes in ANP and BNP expression observed in the $FPR2^{-/-}$ mice.

Additionally, AT-RvD1 reduced cardiac fibrosis in our experimental model. This finding is consistent with that of a previous report showing that the administration of RvD1 to mice infected

519 with *T. cruzi* reduced cardiac fibrosis and transforming growth factor-β (TGF-β) mRNA levels in
520 the heart [19]. However, we used a 20-day continuous treatment scheme during the chronic stage of
521 infection instead of the three-bolus scheme used by the previous investigators. In experimental
522 models of myocardial infarction, RvD1 reduced the transcription of profibrotic genes and decreased
523 collagen deposition, thereby reducing fibrosis and improving ventricular function [59]. The effect of
524 AT-RvD1 on fibrosis is not dependent on FPR2 exclusively since the antifibrotic effect exerted by
525 AT-RvD1 was not impaired in the $FPR2^{-/-}$ mice. Therefore, we propose that GPR32 may be
526 necessary for this purpose, suggesting a level of redundancy within the resolution of the
527 inflammation cascade.

528 An electrocardiographic analysis performed on the infected animals showed alterations in the QT
529 interval in the WT mice, suggesting a slowdown in ventricular repolarization. This alteration
530 appears early in patients with CCC and is a mortality predictor in patients with CD [60, 61].
531 Although this QT interval alteration helped confirm the model's chronic nature, AT-RvD1 did not
532 affect this disease pathology. A more prolonged observation period may be necessary to observe
533 significant AT-RvD1-dependent changes in electrical cardiac function.

534 AT-RvD1 reduces parasite load in *T. cruzi*-infected mice

535 Importantly, AT-RvD1 has no trypanocidal activity. However, we observed that AT-RvD1 alone or
536 combined with Bz reduced the heart parasite load in infected mice. Studies in experimental CCC
537 models have indicated that the administration of 15-epi-LXA_4 similarly reduces the parasite load of
538 cardiac tissue in infected mice [24]. In the absence of FPR2, eliminating the parasite from cardiac
539 tissue is not as efficient, suggesting that the pro-resolving cascade is essential for promoting
540 parasite clearance. Probably, the anti-inflammatory effect of AT-RvD1 reduces the deleterious
541 effect of the inflammatory environment that favors parasite persistence. The pro-resolving processes

initiated by AT-RvD1 enable the immune system to eliminate the parasites, probably because chronic inflammation is an evasive mechanism used by the parasites.

In conclusion, current drug therapies are ineffective in all phases of CD and they do not prevent long-term loss of heart function. Thus, the resolution of inflammation is advantageous as a pharmacological strategy for CCC. FPR2-dependent AT-RvD1 is a pro-resolving lipid mediator effective against inflammation, dampening pathological inflammatory responses and restoring tissue homeostasis; importantly, it contributes to clearing adverse inflammatory environments and allowing more efficient parasite elimination. Consequently, drug strategies aimed to modify host factors and resolve inflammation will improve specific antiparasitic drug therapy in the future.

Acknowledgments

The authors wish to acknowledge grant funding from Agencia Nacional de Investigación y Desarrollo (ANID) FONDECYT grants 1210359 (JDM), 1190341 (UK), 1210627 (GD), 3210667 (SF) and 3180452 (CC); BECAS ANID grant 21170501 (IC), 21170427 (FG) and 21170968 (HQ); Conselho Nacional de Desenvolvimento Científico e Tecnológico (CNPq: 305894/2018-8), and Fundação de Amparo a Pesquisa de Minas Gerais (Rede Mineira de Imunobiológicos, REDE-00140-16) (FSM). In addition, the authors wish to thank Dr. Jader Dos Santos Cruz from the Department of Biochemistry and Immunology, Institute of Biological Sciences, Federal University of Minas Gerais, Brazil, for performing the mouse electrocardiograms.

References:

1. WHO. Chagas disease (also known as American trypanosomiasis). Fact Sheets: WHO 2020: WHO 2020 [cited 2021 August 10]. Available from: https://www.who.int/news-room/fact-sheets/detail/chagas-disease-(american-trypanosomiasis).

2. Coura JR. Chagas disease: what is known and what is needed--a background article. Mem Inst Oswaldo Cruz. 2007;102 Suppl 1:113-22.

3. Perez-Molina JA, Molina I. Chagas disease. Lancet. 2018;391(10115):82-94.

4. Echeverria LE, Morillo CA. American Trypanosomiasis (Chagas Disease). Infect Dis Clin North Am. 2019;33(1):119-34.

5. Rassi A, Jr., Marin JAN, Rassi A. Chronic Chagas cardiomyopathy: a review of the main pathogenic mechanisms and the efficacy of aetiological treatment following the BENznidazole Evaluation for Interrupting Trypanosomiasis (BENEFIT) trial. Mem Inst Oswaldo Cruz. 2017:0.

6. Acevedo GR, Girard MC, Gomez KA. The Unsolved Jigsaw Puzzle of the Immune Response in Chagas Disease. Front Immunol. 2018;9:1929.

7. Bonney KM, Luthringer DJ, Kim SA, Garg NJ, Engman DM. Pathology and Pathogenesis of Chagas Heart Disease. Annu Rev Pathol. 2019;14:421-47.

8. Serhan CN. Discovery of specialized pro-resolving mediators marks the dawn of resolution physiology and pharmacology. Mol Aspects Med. 2017;58:1-11.

9. Serhan CN, Arita M, Hong S, Gotlinger K. Resolvins, docosatrienes, and neuroprotectins, novel omega-3-derived mediators, and their endogenous aspirin-triggered epimers. Lipids. 2004;39(11):1125-32.

10. Serhan CN, Levy BD. Resolvins in inflammation: emergence of the pro-resolving superfamily of mediators. J Clin Invest. 2018;128(7):2657-69.

11. Sun YP, Oh SF, Uddin J, Yang R, Gotlinger K, Campbell E, et al. Resolvin D1 and its aspirin-triggered 17R epimer. Stereochemical assignments, anti-inflammatory properties, and enzymatic inactivation. J Biol Chem. 2007;282(13):9323-34.

12. Serhan CN. Pro-resolving lipid mediators are leads for resolution physiology. Nature. 2014;510(7503):92-101.

13. Lopez-Munoz RA, Molina-Berrios A, Campos-Estrada C, Abarca-Sanhueza P, Urrutia-Llancaqueo L, Pena-Espinoza M, et al. Inflammatory and Pro-resolving Lipids in Trypanosomatid Infections: A Key to Understanding Parasite Control. Front Microbiol. 2018;9:1961.

14. Molina-Berrios A, Campos-Estrada C, Lapier M, Duaso J, Kemmerling U, Galanti N, et al. Protection of vascular endothelium by aspirin in a murine model of chronic Chagas' disease. Parasitol Res. 2013;112(7):2731-9.

15. Carvalho de Freitas R, Lonien SCH, Malvezi AD, Silveira GF, Wowk PF, da Silva RV, et al. Trypanosoma cruzi: Inhibition of infection of human monocytes by aspirin. Exp Parasitol. 2017;182:26-33.

16. Malvezi AD, Panis C, da Silva RV, de Freitas RC, Lovo-Martins MI, Tatakihara VL, et al. Inhibition of cyclooxygenase-1 and cyclooxygenase-2 impairs Trypanosoma cruzi entry into cardiac cells and promotes differential modulation of the inflammatory response. Antimicrob Agents Chemother. 2014;58(10):6157-64.

17. Carlo T, Kalwa H, Levy BD. 15-Epi-lipoxin A4 inhibits human neutrophil superoxide anion generation by regulating polyisoprenyl diphosphate phosphatase 1. FASEB J. 2013;27(7):2733-41. doi: 10.1096/fj.12-223982.

18. Ogata H, Teixeira MM, Sousa RC, Silva MV, Correia D, Rodrigues Junior V, et al. Effects of aspirin-triggered resolvin D1 on peripheral blood mononuclear cells from patients with Chagas' heart disease. Eur J Pharmacol. 2016;777:26-32.

19. Horta AL, Williams T, Han B, Ma Y, Menezes APJ, Tu V, et al. Resolvin D1 Administration Is Beneficial in Trypanosoma cruzi Infection. Infect Immun. 2020;88(6). doi: 10.1128/IAI.00052-20.

20. Pfaffl MW. A new mathematical model for relative quantification in real-time RT-PCR. Nucleic Acids Res. 2001;29(9):e45.

615 21. Soverow J, Hernandez S, Sanchez D, Forsyth C, Flores CA, Viana G, et al. Progression of
616 Baseline Electrocardiogram Abnormalities in Chagas Patients Undergoing
617 Antitrypanosomal Treatment. Open Forum Infect Dis. 2019;6(2):ofz012.
618 22. Marcolino MS, Palhares DM, Ferreira LR, Ribeiro AL. Electrocardiogram and Chagas
619 disease: a large population database of primary care patients. Glob Heart. 2015;10(3):167-
620 72.
621 23. Molina-Berrios A, Campos-Estrada C, Henriquez N, Faundez M, Torres G, Castillo C, et al.
622 Protective role of acetylsalicylic acid in experimental Trypanosoma cruzi infection:
623 evidence of a 15-epi-lipoxin A(4)-mediated effect. PLoS Negl Trop Dis. 2013;7(4):e2173.
624 24. Gonzalez-Herrera F, Cramer A, Pimentel P, Castillo C, Liempi A, Kemmerling U, et al.
625 Simvastatin Attenuates Endothelial Activation through 15-Epi-Lipoxin A4 Production in
626 Murine Chronic Chagas Cardiomyopathy. Antimicrob Agents Chemother. 2017;61(3).
627 25. Esper L, Roman-Campos D, Lara A, Brant F, Castro LL, Barroso A, et al. Role of SOCS2
628 in modulating heart damage and function in a murine model of acute Chagas disease. Am J
629 Pathol. 2012;181(1):130-40.
630 26. Canavaci AM, Sorgi CA, Martins VP, Morais FR, de Sousa EV, Trindade BC, et al. The
631 acute phase of Trypanosoma cruzi infection is attenuated in 5-lipoxygenase-deficient mice.
632 Mediators Inflamm. 2014;2014:893634.
633 27. Pavanelli WR, Gutierrez FR, Mariano FS, Prado CM, Ferreira BR, Teixeira MM, et al. 5-
634 lipoxygenase is a key determinant of acute myocardial inflammation and mortality during
635 Trypanosoma cruzi infection. Microbes Infect. 2010;12(8-9):587-97.
636 28. Cardillo F, de Pinho RT, Antas PR, Mengel J. Immunity and immune modulation in
637 Trypanosoma cruzi infection. Pathog Dis. 2015;73(9):ftv082.
638 29. Ferreira BL, Ferreira ER, de Brito MV, Salu BR, Oliva MLV, Mortara RA, et al. BALB/c
639 and C57BL/6 Mice Cytokine Responses to Trypanosoma cruzi Infection Are Independent
640 of Parasite Strain Infectivity. Front Microbiol. 2018;9:553.

30. Roffe E, Rothfuchs AG, Santiago HC, Marino AP, Ribeiro-Gomes FL, Eckhaus M, et al. IL-10 limits parasite burden and protects against fatal myocarditis in a mouse model of Trypanosoma cruzi infection. J Immunol. 2012;188(2):649-60.

31. Tonelli RR, Torrecilhas AC, Jacysyn JF, Juliano MA, Colli W, Alves MJ. In vivo infection by Trypanosoma cruzi: the conserved FLY domain of the gp85/trans-sialidase family potentiates host infection. Parasitology. 2011;138(4):481-92.

32. Dutra WO, Menezes CA, Magalhaes LM, Gollob KJ. Immunoregulatory networks in human Chagas disease. Parasite Immunol. 2014;36(8):377-87.

33. Machado FS, Martins GA, Aliberti JC, Mestriner FL, Cunha FQ, Silva JS. Trypanosoma cruzi-infected cardiomyocytes produce chemokines and cytokines that trigger potent nitric oxide-dependent trypanocidal activity. Circulation. 2000;102(24):3003-8.

34. Chan CS, Ming-Lum A, Golds GB, Lee SJ, Anderson RJ, Mui AL. Interleukin-10 inhibits lipopolysaccharide-induced tumor necrosis factor-alpha translation through a SHIP1-dependent pathway. J Biol Chem. 2012;287(45):38020-7.

35. Reed SG, Brownell CE, Russo DM, Silva JS, Grabstein KH, Morrissey PJ. IL-10 mediates susceptibility to Trypanosoma cruzi infection. J Immunol. 1994;153(7):3135-40.

36. Anderson CF, Mendez S, Sacks DL. Nonhealing infection despite Th1 polarization produced by a strain of Leishmania major in C57BL/6 mice. J Immunol. 2005;174(5):2934-41.

37. Iyer SS, Cheng G. Role of interleukin 10 transcriptional regulation in inflammation and autoimmune disease. Crit Rev Immunol. 2012;32(1):23-63.

38. Vasconcelos RH, Azevedo Ede A, Diniz GT, Cavalcanti Mda G, de Oliveira W, Jr., de Morais CN, et al. Interleukin-10 and tumour necrosis factor-alpha serum levels in chronic Chagas disease patients. Parasite Immunol. 2015;37(7):376-9.

665 39. Sousa GR, Gomes JA, Fares RC, Damasio MP, Chaves AT, Ferreira KS, et al. Plasma
666 cytokine expression is associated with cardiac morbidity in chagas disease. PLoS One.
667 2014;9(3):e87082.
668 40. Gomes JA, Bahia-Oliveira LM, Rocha MO, Busek SC, Teixeira MM, Silva JS, et al. Type 1
669 chemokine receptor expression in Chagas' disease correlates with morbidity in cardiac
670 patients. Infect Immun. 2005;73(12):7960-6.
671 41. Salas-Hernandez A, Espinoza-Perez C, Vivar R, Espitia-Corredor J, Lillo J, Parra-Flores P,
672 et al. Resolvin D1 and E1 promote resolution of inflammation in rat cardiac fibroblast in
673 vitro. Mol Biol Rep. 2021;48(1):57-66.
674 42. Chen J, Shetty S, Zhang P, Gao R, Hu Y, Wang S, et al. Aspirin-triggered resolvin D1
675 down-regulates inflammatory responses and protects against endotoxin-induced acute
676 kidney injury. Toxicol Appl Pharmacol. 2014;277(2):118-23.
677 43. Bento AF, Claudino RF, Dutra RC, Marcon R, Calixto JB. Omega-3 fatty acid-derived
678 mediators 17(R)-hydroxy docosahexaenoic acid, aspirin-triggered resolvin D1 and resolvin
679 D2 prevent experimental colitis in mice. J Immunol. 2011;187(4):1957-69.
680 44. Lee HN, Kundu JK, Cha YN, Surh YJ. Resolvin D1 stimulates efferocytosis through
681 p50/p50-mediated suppression of tumor necrosis factor-alpha expression. J Cell Sci.
682 2013;126(Pt 17):4037-47.
683 45. Gao Y, Zhang H, Luo L, Lin J, Li D, Zheng S, et al. Resolvin D1 Improves the Resolution
684 of Inflammation via Activating NF-kappaB p50/p50-Mediated Cyclooxygenase-2
685 Expression in Acute Respiratory Distress Syndrome. J Immunol. 2017.
686 46. Fredman G, Ozcan L, Spolitu S, Hellmann J, Spite M, Backs J, et al. Resolvin D1 limits 5-
687 lipoxygenase nuclear localization and leukotriene B4 synthesis by inhibiting a calcium-
688 activated kinase pathway. Proc Natl Acad Sci U S A. 2014;111(40):14530-5.
689 47. Piaggio E, Sanceau J, Revelli S, Bottasso O, Wietzerbin J, Serra E. Trypanocidal drug
690 benznidazole impairs lipopolysaccharide induction of macrophage nitric oxide synthase

gene transcription through inhibition of NF-kappaB activation. J Immunol. 2001;167(6):3422-6.

48. Cevey AC, Mirkin GA, Penas FN, Goren NB. Low-dose benznidazole treatment results in parasite clearance and attenuates heart inflammatory reaction in an experimental model of infection with a highly virulent Trypanosoma cruzi strain. Int J Parasitol Drugs Drug Resist. 2016;6(1):12-22.

49. Garcia S, Ramos CO, Senra JF, Vilas-Boas F, Rodrigues MM, Campos-de-Carvalho AC, et al. Treatment with benznidazole during the chronic phase of experimental Chagas' disease decreases cardiac alterations. Antimicrob Agents Chemother. 2005;49(4):1521-8.

50. Cevey AC, Penas FN, Alba Soto CD, Mirkin GA, Goren NB. IL-10/STAT3/SOCS3 Axis Is Involved in the Anti-inflammatory Effect of Benznidazole. Front Immunol. 2019;10:1267. doi: 10.3389/fimmu.2019.01267.

51. Ribeiro CM, Budni P, Pedrosa RC, Farias MS, Parisotto EB, Dalmarco EM, et al. Antioxidant therapy attenuates oxidative insult caused by benzonidazole in chronic Chagas' heart disease. Int J Cardiol. 2010;145(1):27-33.

52. Hall BS, Wilkinson SR. Activation of benznidazole by trypanosomal type I nitroreductases results in glyoxal formation. Antimicrob Agents Chemother. 2012;56(1):115-23.

53. Morillo CA, Marin-Neto JA, Avezum A, Sosa-Estani S, Rassi A, Jr., Rosas F, et al. Randomized Trial of Benznidazole for Chronic Chagas' Cardiomyopathy. N Engl J Med. 2015;373(14):1295-306.

54. Echeverria LE, Rojas LZ, Calvo LS, Roa ZM, Rueda-Ochoa OL, Morillo CA, et al. Profiles of cardiovascular biomarkers according to severity stages of Chagas cardiomyopathy. Int J Cardiol. 2017;227:577-82.

55. Tucci AR, Oliveira FOR, Jr., Lechuga GC, Oliveira GM, Eleuterio AC, Mesquita LB, et al. Role of FAK signaling in chagasic cardiac hypertrophy. Braz J Infect Dis. 2020;24(5):386-97.

717 56. Corral RS, Guerrero NA, Cuervo H, Girones N, Fresno M. Trypanosoma cruzi infection
718 and endothelin-1 cooperatively activate pathogenic inflammatory pathways in
719 cardiomyocytes. PLoS Negl Trop Dis. 2013;7(2):e2034.
720 57. Petersen CA, Burleigh BA. Role for interleukin-1 beta in Trypanosoma cruzi-induced
721 cardiomyocyte hypertrophy. Infect Immun. 2003;71(8):4441-7.
722 58. Pirault J, Back M. Lipoxin and Resolvin Receptors Transducing the Resolution of
723 Inflammation in Cardiovascular Disease. Front Pharmacol. 2018;9:1273.
724 59. Kain V, Ingle KA, Colas RA, Dalli J, Prabhu SD, Serhan CN, et al. Resolvin D1 activates
725 the inflammation resolving response at splenic and ventricular site following myocardial
726 infarction leading to improved ventricular function. J Mol Cell Cardiol. 2015;84:24-35.
727 60. Salles G, Xavier S, Sousa A, Hasslocher-Moreno A, Cardoso C. Prognostic value of QT
728 interval parameters for mortality risk stratification in Chagas' disease: results of a long-term
729 follow-up study. Circulation. 2003;108(3):305-12.
730 61. Eickhoff CS, Lawrence CT, Sagartz JE, Bryant LA, Labovitz AJ, Gala SS, et al. ECG
731 detection of murine chagasic cardiomyopathy. J Parasitol. 2010;96(4):758-64.
732
733
734